

Mixed integer nonlinear programming for Joint Coordination of Plug-in Electrical Vehicles Charging and Smart Grid Operations

Y. Shi¹, H. D. Tuan¹, and A. V. Savkin²

¹ University of Technology Sydney, Broadway, NSW 2007, Australia
Ye.Shi@student.uts.edu.au, Tuan.Hoang@uts.edu.au,

² The University of New South Wales, Sydney, NSW 2052, Australia
a.savkin@unsw.edu.au

Abstract. The problem of joint coordination of plug-in electric vehicles (PEVs) charging and grid power control is to minimize both PEVs charging cost and energy generation cost, while meeting both residential and PEVs' power demands and suppressing the potential impact of PEVs integration. A bang-bang PEV charging strategy is adopted to exploit its simple online implementation, which requires computation of a mixed integer nonlinear programming problem (MINP) in binary variables of the PEV charging strategy and continuous variables of the grid voltages. A new solver for this MINP is proposed. Its efficiency is shown by numerical simulations.

Key words: Smart grid, plug-in electric vehicles (PEVs), bang-bang charging, mixed integer nonlinear programming

1 Introduction

In recent years, there has been increasing concern over the energy consumption and environment pollution. On the other hand, advance in the battery and smart grid technology have drawn growing attention to electric vehicles (EVs) [1]. It is expected that more than 50% of the new vehicles will be EVs by 2020 [2]. The massive penetration of plug-in electric vehicles (PEVs) can pose potential threats to the stability of a power grid, which is not easily compensated [3]. Unregulated charging of PEVs may cause overloading, additional power loss and unacceptable voltage violation [4]. Coordinate PEV charging is thus needed for the cost-saving services for PEVs and meeting PEV power demands and operation constraints in smart grid system.

To address the coordinate PEV charging problem, [5] proposed a mixed integer nonlinear programming (MINLP) model in an unbalanced system. This MINLP model was then linearized to mixed integer linear programming (MILP) model through the first order Taylor expansion and piecewise linear approximation. As a result, the solution of MILP is not necessarily feasible to the original MINLP problem. Adding a vehicle-to-grid (V2G) charging strategy, similar

MILP model was proposed in [6]. Nevertheless, the practicability of PEVs' discharging involving costs and technologies raised continuous concern in [7]. In addition, the above references for coordinate PEV charging are all based on the off-line strategy. In that case, prior information including the arrival time, departure time and state of charge (SoC) of PEVs must be given beforehand. It is not practical to obtain all of those information in advance. To deal with the online PEV coordination, model predictive control (MPC) approach has been widely used in recent studies [8, 10]. A MPC-based model proposed in [8] scheduled PEV charging in a finite horizon, but operation constraints of grid were not considered. A MILP model over a rolling horizon window for energy storage control was developed in [9] with power balance constraints ignored. Reference [10] proposed a stochastic optimization algorithm to tackle the MILP-based MPC model for different types of PEVs coordination problems, which suffers from large computational cost.

In this paper a bang-bang strategy is adopted for PEV charging. At each time slot individual PEVs either charge at a maximal power rate or do not charge at all. The obvious merit of such bang-bang charging strategy is its easy and efficient online implementation. At each time slot, it requires a joint PEV charging coordination and grid power control for a model predictive system, which is a MINLP in the bang-bang PEV charging variables and the bus voltage variables of the grid. A new approach is developed to handle this MINLP. Firstly, by relaxing the nonlinear constraints of the node voltage variables, the MINLP is convexified to a mixed integer convex programming (MICP). Then we develop a new path-following algorithm for computation of this MICP. The found binary value of the PEV charging coordination is then substituted to the original MINLP for optimizing the bus voltage variables, for which our previously developed nonconvex spectral optimization algorithm [11, 12] is ready for solution. Simulations show that the proposed approach is capable of locating the optimal solution of this MINLP.

The rest of the paper is structured as follows. Section II is devoted to an MINLP-based model for the joint coordination of bang-bang PEV charging and grid power control with analysis on its computational challenges. Section III develops a solver for this MINLP. Simulations are provided in Section IV. Section V concludes the paper.

2 MPC for joint PEV bang-bang charging coordination and grid power control

Like [13], we consider an electric power grid with a set of buses $\mathcal{N} := \{1, 2, \dots, N\}$ connected through a set of flow lines $\mathcal{L} \subseteq \mathcal{N} \times \mathcal{N}$, under which bus k is connected to bus m if and only if $(k, m) \in \mathcal{L}$. Denote by $\mathcal{N}(k)$ the set of other buses connected to bus k . $\mathcal{G} \subseteq \mathcal{N}$ is the set of those buses that are connected to distributed generators (DGs). Bus $k \in \mathcal{N} \setminus \mathcal{G}$ is not connected to DGs and bus $k \in \mathcal{G}$ also has a function to serve PEVs and will be referred as charging station

(CS) k . Thus, there are $M = |\mathcal{G}|$ CSs in the grid. The serving time period of the grid is divided into T time slots $\mathcal{T} := \{1, 2, \dots, T\}$.

Denote by \mathcal{H}_k the set of those PEVs that arrive at CS k . Accordingly, k_n is the n -th PEV that arrives at CS k . Each PEV k_n arrives at $t_{a,k_n} \in \mathcal{T}$ and requires to be fully charged by its departing time $t_{k_n,d} \in \mathcal{T}$. Suppose that C_{k_n} and $s_{k_n}^0$ are the battery capacity and initial SOC of PEV k_n while \bar{P}_{k_n} is the maximum power that its battery can charge during one time slot. In this paper, we adopt the bang-bang charging strategy, under which PEV k_n either charges the maximal power \bar{P}_{k_n} or does not charge at all at each time slot. We use the binary variable

$$\tau_{k_n}(t') \in \{0, 1\} \quad (1)$$

to implement this strategy, i.e. PEV k_n charges the power $P_{k_n}(t') = \tau_{k_n}(t')\bar{P}_{k_n}$ during the time slot t' . Accordingly, the following constraint enables PEV k_n to be fully charged at its departure:

$$\sum_{t'=t_{k_n,a}}^{t_{k_n,d}} \tau_{k_n}(t') = \bar{\tau}_{k_n}, \quad (2)$$

where u_h is the charging efficiency of the battery, $\bar{\tau}_{k_n} := \lceil \frac{C_{k_n}(1-s_{k_n}^0)}{u_h \bar{P}_{k_n}} \rceil$. For ease of presentation, we set $\tau_{k_n}(t') = 0$ for $t' \notin [t_{k_n,a}, t_{k_n,b}]$.

From the grid side, let $y_{km} \in \mathbb{C}$ be the admittance of line (k, m) , The current $I_k(t')$ at node $k \in \mathcal{N}$ is $V_k(t')$ is the complex voltage at bus k during the time slot t' , the total supply and demand energy is balanced as:

$$V_k(t') \left[\sum_{m \in \mathcal{N}(k)} y_{km} (V_k - V_m) \right]^* = [P_{g_k}(t') - P_{l_k}(t') - \sum_{n \in \mathcal{H}_k} \bar{P}_{k_n} \tau_{k_n}(t')] + j[Q_{g_k}(t') - Q_{l_k}(t')], \quad k \in \mathcal{G}, \quad (3)$$

$$V_k(t) \left[\sum_{m \in \mathcal{N}(k)} y_{km} (V_k - V_m) \right]^* = -P_{l_k}(t') - jQ_{l_k}(t'), \quad k \in \mathcal{N} \setminus \mathcal{G}, \quad (4)$$

where $P_{l_k}(t')$ and $Q_{l_k}(t')$ are respectively known real and reactive price-inelastic demands to express the residential power demand, $P_{g_k}(t')$ and $Q_{g_k}(t')$ are the real and reactive powers generated by DG k .

The following standard constraints are also set.

– The range of generated powers by the DGs:

$$\underline{P}_{g_k} \leq P_{g_k}(t') \leq \bar{P}_{g_k}, \quad \underline{Q}_{g_k} \leq Q_{g_k}(t') \leq \bar{Q}_{g_k}, \quad k \in \mathcal{G}, \quad (5)$$

where \underline{P}_{g_k} , \underline{Q}_{g_k} and \bar{P}_{g_k} , \bar{Q}_{g_k} are respectively lower and upper physical limits of the real generated and reactive generated powers.

– Voltage range and phase balance:

$$\underline{V}_k \leq |V_k(t')| \leq \bar{V}_k, \quad |\arg(V_k(t')) - \arg(V_m(t'))| \leq \theta_{km}^{\max}, \quad (6)$$

$$k \in \mathcal{N}, (k, m) \in \mathcal{L}, t' \in \mathcal{T},$$

where \underline{V}_k and \bar{V}_k are the lower limit and upper limit of the voltage amplitude, while $\theta_{k,m}^{\max}$ are given to express the voltage phase balance.

The cost function is defined as the sum of the energy cost to DGs and charging cost for PEVs

$$\mathcal{F}(\mathcal{R}, \tau) = \sum_{t' \in \mathcal{T}} \sum_{k \in \mathcal{G}} f(P_{g_k}(t')) + \sum_{t' \in \mathcal{T}} \sum_{k \in \mathcal{N}} \sum_{n \in \mathcal{H}_k} \beta_t \tau_{k_n}(t') \bar{P}_{k_n}, \quad (7)$$

where $f(P_{g_k}(t'))$ is the cost function of real power generation by DGs, which is linear or quadratic in $P_{g_k}(t')$, and β_t is the known PEV charging price during the time slot t' .

By defining $R(t') = \{P_g(t'), Q_g(t')\}$, $\mathcal{R} = \{R(t')\}_{t' \in \mathcal{T}}$, and $\tau = \{\tau(t')\}_{t' \in \mathcal{T}}$, $\tau(t') = \{\tau_{k_n}(t')\}_{k_n \in \mathcal{H}_k}$, $(R(t'), \tau^{PEV}(t'))$ and $V(t')$ are considered as the system state and control, respectively. As such, the joint PEV charging coordination and voltage control to optimize the energy and charging costs appears to be the following control problem over the finite horizon $[1, T]$:

$$\min_{\mathcal{V}, \mathcal{R}, \tau^{PEV}} \mathcal{F}(\mathcal{R}, \tau^{PEV}) \quad \text{s.t.} \quad (1), (2), (3) - (6). \quad (8)$$

However, all equations in (8) are not known a priori.

Denote by $C(t)$ the set of PEVs that need to be charged at t and ahead. For each $k_n \in C(t)$, let $d_{k_n}(t)$ be its remaining demand for charging by the departure time $t_{k_n, d}$. Therefore, the binary variable

$$\tau_{k_n}(t') \in \{0, 1\}, t' \in [t, t_{k_n, d}], k_n \in C(t) \quad (9)$$

must satisfy the following constraints:

$$\sum_{t'=t}^{t_{k_n, d}} \tau_{k_n}(t') = \bar{\tau}_{k_n}(t), k_n \in C(t), \quad (10)$$

where $\bar{\tau}_{k_n}(t) := \lceil \frac{d_{k_n}(t)}{u_h P_{k_n}} \rceil$. Define $\Psi(t) = \max_{k_n \in C(t)} t_{k_n, d}$, we propose an online algorithm, which at time t solves the following MPC over the prediction horizon $[t, \Psi(t)]$ but then takes only $V(t)$, $R(t)$ and $\tau(t)$, for updating the solution of (8):

$$\begin{aligned} & \min_{\mathcal{V}_P(t), \mathcal{R}_P(t), \tau_P(t)} F_P(\mathcal{R}_P(t), \tau_P(t)) \quad \text{s.t.} \quad (4) - (6), (9), (10), \\ & V_k(t') \left[\sum_{m \in \mathcal{N}(k)} y_{km} (V_k(t') - V_m(t')) \right]^* = [P_{g_k}(t') - P_{l_k}(t') \\ & - \sum_{k_n \in C(t)} \bar{P}_{k_n} \tau_{k_n}(t')] + j(Q_{g_k}(t') - Q_{l_k}(t')), \quad (t', k) \in [t, \Psi(t)] \times \mathcal{G}. \quad (11a) \end{aligned}$$

One can see (11) is a difficult MINP because (4), (6) and (11a) are nonlinear in the voltage variable $V(t')$ while (9) is a discrete combinatoric constraint. In the next section, we propose an efficient approach, which also exploits the fact that only the snapshot at t of the solution of (11) is extracted to update the online solution of (8).

3 Solver for MINP

For $W(t') := V(t')V^H(t') \in \mathbb{C}^{N \times N}$, which must satisfy $W(t') \succeq 0$ and $\text{rank}(W(t')) = 1$, we replace $W_{km}(t') = V_k(t')V_m^*(t')$, $(k, m) \in \mathcal{N} \times \mathcal{N}$ in, in (11) to reformulate it to the following MINP in matrix-valued variable $\mathcal{W}_P(t) := \{W(t')\}_{t' \in [t, \Psi(t)]}$ and binary-valued variable $\tau_P(t)$:

$$\begin{aligned} \min_{\mathcal{W}_P(t), \mathcal{R}_P(t), \tau_P(t)} F_P(\mathcal{R}_P(t), \tau_P(t)) \quad \text{s.t. (5), (9), (10),} \\ \sum_{m \in \mathcal{N}(k)} (W_{kk}(t') - W_{km}(t'))y_{km}^* = [P_{g_k}(t') - P_{l_k}(t') \\ - \sum_{k_n \in C(t)} \bar{P}_{k_n} \tau_{k_n}(t')] + j(Q_{g_k}(t') - Q_{l_k}(t')), \quad k \in \mathcal{G}, \end{aligned} \quad (12a)$$

$$\sum_{m \in \mathcal{N}(k)} (W_{kk}(t') - W_{km}(t'))y_{km}^* = -P_{l_k}(t') - jQ_{l_k}(t'), k \notin \mathcal{G}, \quad (12b)$$

$$\underline{V}_k^2 \leq W_{kk}(t') \leq \bar{V}_k^2, \quad k \in \mathcal{N}, \quad (12c)$$

$$\Im(W_{km}(t')) \leq \Re(W_{km}(t')) \tan(\theta_{km}^{max}), (k, m) \in \mathcal{L}, \quad (12d)$$

$$W(t') \succeq 0, \quad (12e)$$

$$\text{rank}(W(t')) = 1, \quad (12f)$$

The difficulty of (12) is concentrated on the multiple nonconvex matrix rank-one constraints in (12f) and multiple binary constraints in (9). Below we propose a two-stage optimization approach to its online algorithm. In the first optimization stage, we drop the matrix rank-one constraint (12f) to relax (12) to the following MIPC for $t' \in [t, \Psi(t)]$:

$$\min_{\mathcal{W}_P(t), \mathcal{R}_P(t), \tau_P(t)} F_P(\mathcal{R}_P(t), \tau_P(t)) \quad \text{s.t. (5), (9), (10), (12a) - (12e)}. \quad (13)$$

Suppose that $(\hat{\mathcal{W}}_P(t), \hat{\mathcal{R}}_P(t))$ and $\hat{\tau}_P(t)$ is the optimal solution of (13). If $\text{rank}(\hat{W}(t')) \equiv 1$, $t' \in [t, \Psi(t)]$, then $\hat{V}(t')$ such that $\hat{W}(t') = \hat{V}(t')\hat{V}^H(t')$ together with $\hat{R}(t')$ and $\hat{\tau}_{k_n}(t')$ constitute the optimal solution of MINP (11). Otherwise, we go to the next optimization stage, which substitutes $\hat{\tau}_{k_n}(t)$ into (12a) to consider the snapshot at t of (12) only

$$\min_{W(t), R(t)} F(P_g(t)) := \sum_{t'=t}^{\Psi(t)} \sum_{k \in \mathcal{G}} f(P_{g_k}(t')) \quad \text{s.t. (5), (12b) - (12e)} \quad (14a)$$

$$\begin{aligned} \sum_{m \in \mathcal{N}(k)} (W_{kk}(t) - W_{km}(t))y_{km}^* = [P_{g_k}(t) - P_{l_k}(t) \\ - \sum_{k_n \in C(t)} \bar{P}_{k_n} \hat{\tau}_{k_n}(t)] + j(Q_{g_k}(t) - Q_{l_k}(t)), \quad k \in \mathcal{G}, \end{aligned} \quad (14b)$$

$$\text{rank}(W(t)) = 1, \quad (14c)$$

which involves only one matrix rank-one constraint (14c). The rationale behind this simplified treatment is that in the end we need only the snapshot at t of the solution of (12) for online updating the voltage $V(t)$ and generated power $R(t)$.

In the next two subsections we propose algorithms for solving MICP (13) and the nonconvex optimization problem (14).

3.1 New computational solution for MICP problem (13)

It is clear that the main task is how to cope with the discrete constraint (9) in MICP (13). The following result establishes the equivalence between this discrete constraint and a set of continuous constraints.

Lemma 1 *Under the linear constraint (10), the binary constraint (9) is equivalent to the following set of continuous constraints:*

$$0 \leq \tau_{k_n}(t') \leq 1, t' \in [t, t_{k_n,d}], k_n \in C(t), \quad (15)$$

$$g(\tau_P(t)) \geq \bar{\tau}(t) := \sum_{k_n \in C(t)} \bar{\tau}_{k_n}(t), \quad (16)$$

where $g(\tau_P(t)) := \sum_{k_n \in C(t)} \sum_{t'=t} t_{k_n,b} \tau_{k_n}^L(t')$, for $L > 1$.

The following result is a direct consequence of Lemma 1.

Proposition 1 *Under the linear constraint (10), the function*

$$g_1(\tau_P(t)) := \frac{1}{g(\tau_P(t))} - \frac{1}{\bar{\tau}(t)}$$

can be used to measure the degree of satisfaction of the binary constraint (9) in the sense that $g_1(\tau_P(t)) \geq 0 \forall \tau_{k_n}(t') \in [0, 1]$ and $g_1(\tau_P(t)) = 0$ if and only if $\tau_{k_n}(t')$ are binary (i.e. satisfying (9)).

Therefore MICP (13) is equivalent to the following penalized optimization problem:

$$\begin{aligned} \min_{\mathcal{W}_P(t), \mathcal{R}_P(t), \tau_P(t)} \quad & \Phi(\mathcal{R}_P(t), \tau_P(t)) := F_P(\mathcal{R}_P(t), \tau_P(t)) + \mu g_1(\tau_P(t)) \\ \text{s.t.} \quad & (5) \text{ for } t' \in [t, \Psi(t)], (10), (12a) - (12e), (15), \end{aligned} \quad (17)$$

where $\mu > 0$ is a penalty parameter. As the function $g(\tau_P(t))$ is convex, it is true that at $\tau_P^{(\kappa)}(t)$ [15],

$$\begin{aligned} g(\tau_P(t)) &\geq g^{(\kappa)}(\tau_P(t)) \\ &:= g(\tau_P^{(\kappa)}(t)) + \langle \nabla g(\tau_P^{(\kappa)}(t)), \tau_P(t) - \tau_P^{(\kappa)}(t) \rangle \\ &= -(L-1) \sum_{k_n \in C(t)} \sum_{t'=t}^{t_{k_n,d}} (\tau_{k_n}^{(\kappa)}(t'))^L + L \sum_{k_n \in C(t)} \sum_{t'=t}^{t_{k_n,d}} (\tau_{k_n}^{(\kappa)}(t'))^{L-1} \tau_{k_n}(t'). \end{aligned} \quad (18)$$

Therefore, an upper bounding approximation at $\tau_P^{(\kappa)}(t)$ for $g_1(\tau_P(t))$ can be easily obtained as

$$g_1(\tau_P(t)) \leq g_1^{(\kappa)}(\tau_P(t)) := \frac{1}{g^{(\kappa)}(\tau_P(t))} - \frac{1}{\bar{\tau}(t)} \quad (19)$$

over the trust region

$$g^{(\kappa)}(\tau_P(t)) > 0. \quad (20)$$

Accordingly, at the κ -th iteration we solve the following convex optimization problem to generate the next iterative point $(\mathcal{W}_P^{(\kappa+1)}(t), \mathcal{R}_P^{(\kappa+1)}(t), \tau_P^{(\kappa+1)}(t))$:

$$\begin{aligned} \min_{\mathcal{W}_P(t), \mathcal{R}_P(t), \tau_P(t)} \quad & \Phi^{(\kappa)}(\mathcal{R}_P(t), \tau_P(t)) := F_P(\mathcal{R}_P(t), \tau_P(t)) + \mu g_1^{(\kappa)}(\tau_P(t)) \\ \text{s.t.} \quad & (5), \quad \text{for } t' \in [t, \Psi(t)], (10), (12a) - (12e), (15), (20). \end{aligned} \quad (21)$$

We thus arrive at $\Phi(\mathcal{R}_P^{(\kappa+1)}(t), \tau_P^{(\kappa+1)}(t)) \leq \Phi^{(\kappa)}(\mathcal{R}_P^{(\kappa+1)}(t), \tau_P^{(\kappa+1)}(t)) < \Phi^{(\kappa)}(\mathcal{R}_P^{(\kappa)}(t), \tau_P^{(\kappa)}(t)) = F(\mathcal{R}_P^{(\kappa)}(t), \tau_P^{(\kappa)}(t))$, implying that $\tau_P^{(\kappa+1)}(t)$ is a better feasible point than $\tau_P^{(\kappa)}(t)$ for (17). For a sufficiently large $\mu > 0$, $g(\tau_P^{(\kappa)}(t)) \rightarrow 0$ as well, yielding an optimal solution of MICP (13). Pseudo-code for this computational procedure is provided by Algorithm 1.

Algorithm 1 MICP Solver

Initialization. Choose a feasible point $\tau_P^{(0)}(t)$ for (17) as the optimal solution of the following problem by relaxing the binary constraints (9) in (13) to box constraints:

$$\min_{\mathcal{W}_P(t), \mathcal{R}_P(t), \tau_P(t)} F_P(\mathcal{R}_P(t), \tau_P(t)) \text{ s.t. } (5), (12a) - (12e), (10), \tau_{k_n}(t') \in [0, 1], \quad (22)$$

Set $\kappa = 0$.

κ -th iteration. Solve (21). If the optimal solution $\tau_P^{(\kappa+1)}(t)$ satisfies $\sum_{k_n \in C(t)} \sum_{t'=t}^{t_{k_n, d}} \left(\tau_{k_n}^{(\kappa+1)}(t') - \left(\tau_{k_n}^{(\kappa+1)}(t') \right)^L \right) \approx 0$, terminate the algorithm and output $\tau_P^{(\kappa+1)}(t)$ as a found solution. Otherwise, reset $\kappa + 1 \rightarrow \kappa$ and $\tau_P^{(\kappa+1)}(t) \rightarrow \tau_P^{(\kappa)}(t)$ for the next iteration.

3.2 Computational procedure for (14)

Following our previous works [11, 12, 14, 16, 17], the matrix rank-one constrained optimization problem (14) is solved via the following penalized optimization problem for $\lambda > 0$:

$$\min_{W(t), R(t)} F(P_g(t)) + \lambda(\text{Trace}(W(t)) - \lambda_{\max}(W(t))), \quad (23a)$$

$$\text{s.t. } (5), (12b) - (12e) \quad \text{for } t' = t, \quad (23b)$$

which is computed by solving the following convex optimization problem at the κ th iteration to generate $W^{(\kappa+1)}(t)$:

$$\begin{aligned} \min_{W(t), R(t)} \quad & F(P_g(t)) + \lambda(\text{Trace}(W(t))) \\ & -(w_{\max}^{(\kappa)}(t))^H W(t) w_{\max}^{(\kappa)}(t) \quad \text{s.t.} \quad (23b), \end{aligned} \quad (24)$$

where $W^{(k)}(t)$ is a point found from the $(\kappa - 1)$ th iteration and $w_{\max}^{(\kappa)}(t)$ denotes the normalized eigenvector corresponding to the maximal eigenvalue $\lambda_{\max}(W^{(\kappa)}(t))$ of $W^{(\kappa)}(t)$. The rationale behind using the penalized optimization problem (23) is that $\text{Trace}(W(t)) - \lambda_{\max}(W(t))$ is the degree of satisfaction of the matrix rank-one constraint (14c). The reader is referred to [12] for proof of its convergence.

4 Simulation results

Sedumi [18] solver under the framework of CVX [19] on a Core i7-7600U processor is used to solve convex optimization problems such as (21) and (24). Simulations are tested on IEEE-30 network, whose structure, physical limits and cost functions $f(P_{g_k}(t'))$ are provided in the Matpower library [20].

The considered charging period is from 6:00 pm to 6:00 am of the next day to reflect the fact that most PEVs are charged after their owners' working hours. This time period is uniformly divided into 24 30-minute time slots. The PEVs arrive during the time period from 6:00 pm to midnight. The arrival times of PEVs are independent and are generated by a truncated normal distribution $(8, 1.5^2)$. The battery capacity $C_{k_n} = 100$ KWh of PEVs is that of Tesla Model S. The initial SOC $s_{k_n}^0$ of all PEVs is set as 20%.

The price-inelastic load $P_{l_k}(t)$ is defined as $P_{l_k}(t) = l(t) \times \bar{P}_{l_k} \times T / \sum_{t=1}^{24} l(t)$, where \bar{P}_{l_k} is the load demand specified by [20] and $l(t)$ is the residential load demand taken from the UK [21]. The time varying energy price is taken from [22] on different days in 2017. The tolerance $\epsilon = 10^{-4}$ is set for the stop criteria and $L = 1.5$ in (18) is chosen to accelerate the convergence speed for the optimization algorithms.

The computational results are summarized in Table 1. Its third column pro-

Table 1. Online bang-bang charging computational results

Networks	Profiles	Binary variables	μ	λ	Obj. (7) by (13)	Obj. (7) by (14)	Time (s)
Case30	Profile 1	3012	10	1	6560.7	6560.8	24.0
	Profile 2	3012	10	1	6569.6	6569.7	23.1
	Profile 3	3012	10	1	6615.1	6615.2	25.2
	Profile 4	3012	10	1	6589.3	6599.1	29.4

vides the number of binary variables $\tau_{k_n}(t')$ in (8). The values of the penalty

parameters μ in (21) and λ in (24) are specified in the forth and fifth columns. The value of the cost objective (7) by (13) and (14) are given by the sixth and seventh columns, respectively. The effectiveness of using (14) is confirmed by observing that these values are almost the same. The average running time of computation at each time slot is shown in the last column.

Fig.1 plot the SoC of four PEVs randomly taken from simulation on profile 3, which arrive at different times. For a few time slots, PEVs do not charge so their SoC remain unchanged.

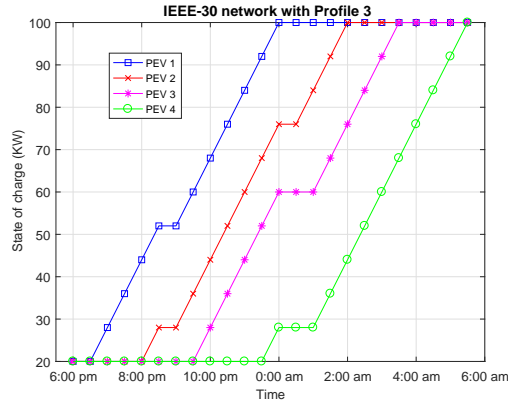


Fig. 1. The SOC of PEVs during the charging period

5 Conclusions

The joint online coordination of PEV bang-bang charging and power control to serve both PEVs at a competitive cost and residential power demands at a competitive operating cost is very difficult due to the random nature of PEVs' arrivals and demands and the discrete nature of bang-bang charging. We have proposed a novel and easily-implemented MPC-based two-optimization stage online algorithm that can achieve an optimal solution.

References

1. Edison Electric Institute: Transportation electrification: Utility fleets leading the charge (white paper), EEL, (2014)
2. Scrosati, Bruno and Garcke, Jürgen and Tillmetz, Werner: Advances in battery technologies for electric vehicles, Woodhead Publishing, (2015)
3. S. Lakshminarayana, Y. Xu, H. V. Poor, T. Q. S. Quek: Cooperation of storage operation in a power network with renewable generation, IEEE Trans. Smart Grid, vol. 7, no. 4, pp. 2108–2122, (2016)

4. S. Huang, H. Safiullah, J. Xiao, B.-M. S. Hodge, R. Hoffman, J. Soller, D. Jones, D. Dinninger, W. E. Tyner, A. Liu, et al.: The effects of electric vehicles on residential households in the city of indianapolis, *Energy Policy*, vol. 49, pp. 442–455, (2012)
5. J. F. Franco, M. J. Rider, and R. Romero: A mixed-integer linear programming model for the electric vehicle charging coordination problem in unbalanced electrical distribution systems, *IEEE Trans. Smart Grid*, vol. 6, no. 5, pp. 2200–2210, (2015)
6. C. S. Antnez, J. F. Franco, M. J. Rider, R. Romero, A new methodology for the optimal charging coordination of electric vehicles considering vehicle-to-grid technology, *IEEE Trans. Sustainable Energy*, vol. 7, pp. 596–607, April (2016)
7. K. Clement-Nyns, E. Haesen, J. Driesen: The impact of vehicle-to-grid on the distribution grid, *Electric Power Systems Research*, vol. 81, no. 1, pp. 185–192, (2011)
8. W. Tang and Y. J. A. Zhang: A model predictive control approach for low-complexity electric vehicle charging scheduling: optimality and scalability, *IEEE Trans. Power Systems*, vol. 32, no. 2, pp. 1050–1063, (2017)
9. P. Malysz, S. Sirouspour, A. Emadi: An optimal energy storage control strategy for grid-connected microgrids, *IEEE Trans. Smart Grid*, vol. 5, pp. 1785–1796, (2014)
10. A. Ravichandran, S. Sirouspour, P. Malysz, A. Emadi: A chance-constraints-based control strategy for microgrids with energy storage and integrated electric vehicles, *IEEE Trans. Smart Grid*, (2016)
11. A. H. Phan, H. D. Tuan, H. H. Kha, D. T. Ngo: Nonsmooth optimization for efficient beamforming in cognitive radio multicast transmission, *IEEE Trans. Sign. Process.*, vol. 60, no. 6, pp. 2941–2951, (2012)
12. Y. Shi, H. D. Tuan, H. Tuy, S. Su: Global optimization for optimal power flow over transmission networks, *J. Global Optimz.* vol. 69, pp. 745–760, (2017)
13. Y. Shi, H. D. Tuan, A. V. Savkin, T. Q. Duong, H. V. Poor: Model predictive control for smart grids with multiple electric-vehicle charging stations, [Online]. <http://arxiv.org/abs/1708.07626>.
14. Y. Shi, H. D. Tuan, P. Apkarian: Nonconvex spectral optimization algorithms for reduced-order H_∞ LPV-LFT controllers, *Int. J. Non. Robust Control*, vol. 27, pp. 4421–4442, (2017)
15. H. Tuy: *Convex Analysis and Global Optimization* (second edition). Springer International Publishing AG, (2017)
16. Y. Shi, H. D. Tuan, S. W. Su, H. H. M. Tam: Nonsmooth optimization for optimal power flow over transmission networks, in 2015 IEEE Global Conf. Signal Info. Process. (GlobalSIP), pp. 1141–1144, (2015)
17. A. A. Nasir, H. D. Tuan, D. T. Ngo, T. Q. Duong, H. V. Poor: Beamforming design for wireless information and power transfer systems: Receive power-splitting versus transmit time-switching, *IEEE Trans. Commun.*, vol. 65, no. 2, pp. 876–889, (2017)
18. J. Sturm: Using SeDuMi 1.02, a MATLAB toolbox for optimization over symmetric cones, *Optimization Methods and Software*, vol. 11-12, pp. 625–653, (1999)
19. M. Grant, S. Boyd: CVX: Matlab software for disciplined convex programming, version 2.1. <http://cvxr.com/cvx>.
20. R. D. Zimmerman, C. E. Murillo-Sanchez, and R. J. Thomas: Matpower: Steady-state operations, planning, and analysis tools for power systems research and education, *IEEE Trans. Power Systems*, vol. 26, pp. 12–19, (2011)
21. The residential demand of the UK. <http://www.gridwatch.templar.co.uk/download.php>.
22. The electricity price of the uk. <https://www.businesselectricityprices.org.uk/retail-versus-wholesale-prices/>.